

Study of Reactions Induced in Be⁹ by 46-MeV Protons*

J. W. VERBA, H. WILLMES, R. F. CARLSON, I. ŠLAUS,† J. REGINALD RICHARDSON, AND E. L. PETERSEN‡

University of California, Los Angeles, California

(Received 12 September 1966)

Reactions induced by the bombardment of Be⁹ by 46-MeV protons have been studied. Angular distributions have been measured for Be⁹(*p,p*)Be⁹ (elastic scattering), Be⁹(*p,p'*)Be^{9*} (2.43-MeV state), Be⁹(*p,d*)Be⁸ (ground state), Be⁹(*p,d*)Be^{8*} (2.90-MeV state), Be⁹(*p,d*)Be^{8*} (16.93-MeV state), Be⁹(*p,d*)Be^{8*} (17.64-MeV state), Be⁹(*p,d*)Be^{8*} (18.15-MeV state), Be⁹(*p,d*)Be^{8*} (19.05-MeV state), Be⁹(*p,t*)Be⁷ (ground state), Be⁹(*p,t*)Be^{7*} (4.55-MeV state), Be⁹(*p,t*)Be⁷ (6.51-MeV state), and Be⁹(*p,t*)Be^{7*} (10.79-MeV state).

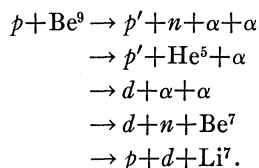
I. INTRODUCTION

THERE is some hope that a nucleus as light as Be⁹ will eventually be amenable to an exact treatment, i.e., that all of its properties will be predictable from knowledge of the nuclear forces. In a sense, this hope is strengthened when one realizes that Be⁹ can be quite well described as the three-body system

$$\text{Be}^9 = \alpha + \alpha + n.$$

On the other hand, Be⁹ is heavy enough so that nuclear models may be applicable. For example, the collective model has been quite successful in describing the level structure of Be⁹, and the optical model seems to adequately describe nuclear scattering from Be⁹.

This dichotomy of approach applies to the region of nuclei with mass number $6 \leq A \leq 16$. The common characteristic of these nuclei is a small value for the separation energies. For example, the nucleus Be⁸ is unstable with respect to the decay into two alpha particles, the He³+He⁴ system is only 1.587 MeV higher in energy than is Be⁷, the binding energy of the last neutron in Be⁹ is only 1.666 MeV, etc. As a consequence, nuclear reactions leading to such nuclei often result in a breakup into more than two particles; some examples are



Although these breakup processes merit their own investigation, their very existence implies that the groups corresponding to the reactions leaving such nuclei (as Be⁷, Be⁸, Be⁹, etc.) in their various excited levels are superimposed upon the continuous breakup spectra.

The small binding energy of the last neutron in Be⁹ results in a high probability of the neutron being well outside the range of the nuclear forces. For a square well

of radius 3 F for example, the neutron has a 56% probability of being outside the range of the nuclear forces and a 25% chance of being further than 5 F from the center of the nucleus.

Nuclear reactions involving beryllium isotopes have been the subject of many investigations. The elastic scattering of protons by Be⁹ has been studied at proton energies of 6, 5 to 15, 8, 10, 12, 18.9, 19.5, 20, 31, 31.5, 142, 143, 160, 316, and 725 MeV.¹ Differential cross sections have been measured for Be⁹(*p,p'*)Be^{9*} for transitions to the 2.43-, 4.8-, and 6.66-MeV levels¹⁻³; angular distributions related to other levels of Be⁹ have not as yet been reported. Spectra resulting from the inelastic scattering of protons, deuterons, alpha particles, and electrons from Be⁹ performed at various energies up to 300 MeV show a striking similarity; namely, the levels at 2.43 and 6.66 MeV in Be⁹ are strongly excited, while the other levels are not.¹ There is strong evidence that the 2.43- and the 6.66-MeV levels are collective states; the excitation energies, the transition widths, and essentially all of the data available for these two levels can be explained by assuming that they are the $\frac{5}{2}-$ and $\frac{7}{2}-$ members of the $K = \frac{3}{2}-$ rotational band based on the ground state. Assuming the same moment of inertia, the $\frac{3}{2}-$ member is expected in the region of 10 to 11 MeV; the 11.3-MeV level is a good candidate. The similarity between the inelastic scattering induced by protons, deuterons, and alpha particles suggests that the spin-dependent part of the nuclear interaction makes a relatively minor contribution to the inelastic cross section.¹

The reaction Be⁹(*p,d*)Be⁸ has been studied at proton energies from 5 to 155 MeV.¹ The deuteron spectra reveal groups corresponding to the Be⁸ ground state, the 2.9-MeV state, and peaks which can be associated with levels around 17 and 19 MeV. The pronounced group in the vicinity of 17 MeV has been identified as the 16.9-MeV level.⁴ It is interesting to remark that the angular distributions of the ground-state group are

¹ T. Lauritsen and F. Ajzenberg-Selove, Nucl. Phys. **78**, 1 (1966).

² G. Schrank, E. K. Warburton, and W. W. Daehnick, Phys. Rev. **127**, 2159 (1962).

³ D. Hasselgren, P. U. Renberg, O. Sundberg, and G. Tibell, Nucl. Phys. **69**, 81 (1965).

⁴ T. H. Short, thesis, University of Minnesota, 1965 (unpublished).

* Supported in part by the Office of Naval Research, Contract Nonr 233-(44).

† On leave of absence from Institute "R. Bosković," Zagreb, Yugoslavia.

‡ Present address: San Fernando Valley State College, Northridge, California.

substantially identical throughout the range of incident proton energies of 5 to 30 MeV; this presents an example of a failure of the simple Butler theory with a fixed cutoff radius. It has been argued that the transparent-nucleus Born-approximation pickup theory gives a better description of the process.⁵

The highly excited levels of Be⁸ have recently attracted some attention. It was pointed out by Marion⁶ that the 16.63-MeV and the 16.93-MeV levels have particularly pure single-particle configurations, namely, 16.6-MeV level: $p+Li^7$ (ground state), $J^\pi=2^+$ and 16.9-MeV level: $n+Be^7$ (ground state), $J^\pi=2^+$, and that the description of these levels in terms of isospin is inappropriate. It is possible that the levels at 17.64 MeV and 18.15 MeV have similar structure⁶; i.e., 17.64-MeV level: $p+Li^{7*}$ (0.478-MeV level) and 18.15-MeV level: $n+Be^{7*}$ (0.43-MeV level). Thus, the pair of levels with the lower energies (16.63, 16.93 MeV) would be the result of a coupling between a nucleon and the $A=7$ ground-state core, while the higher energy pair of levels (17.64 MeV, 18.15 MeV) would be a configuration of a nucleon and either Li⁷ or Be⁷ in their first excited states.

The (p,t) and (p,He^3) reactions represent a valuable tool in nuclear spectroscopy. Specifically, it has been shown that they might help to identify states of high isospin in the residual nuclei.⁷ The Be⁹ (p,t) Be⁷ reaction has been studied at 44 MeV with the aim of determining the $T=\frac{3}{2}$ levels in the $A=7$ nuclei.⁸ Triton groups were observed, corresponding to transitions to the ground state, the 0.43-MeV, the 4.55-MeV, and 10.79-MeV states of Be⁷. The 10.79-MeV level, a new level, was identified by Detraz *et al.* as the lowest $T=\frac{3}{2}$ level in Be⁷.

II. EXPERIMENTAL ARRANGEMENT

A. Proton Beam

The experiment was performed using the proton beam from the University of California at Los Angeles sector-focused cyclotron. The proton beam is obtained by accelerating negative hydrogen ions; extraction from the cyclotron is accomplished by passing the ions through a 0.0005-in.-thick beryllium foil, which strips off the two electrons from each ion. This method results in essentially 100% extraction of a beam of small divergence.

A schematic drawing of the experimental area is shown in Fig. 1. After the protons are extracted from the cyclotron, they pass, while still in the cyclotron vault, through a quadrupole doublet; the result is a waist in the beam cross section, occurring just outside

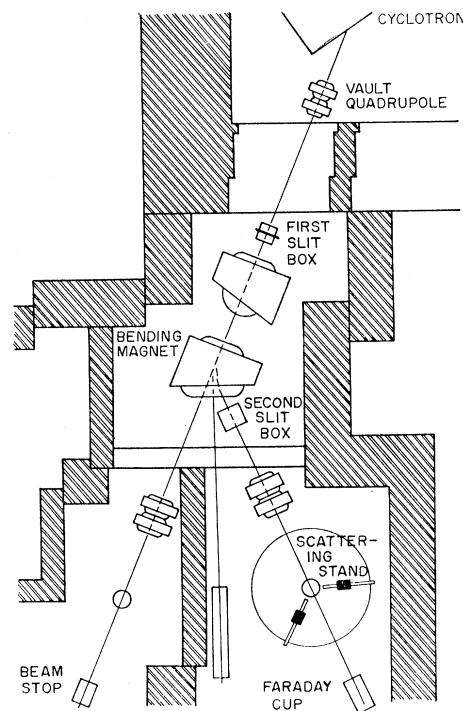


FIG. 1. Schematic drawing of the experimental area.

the vault wall. A set of remotely adjustable copper slits is located at the position of the waist; these slits are set to transmit about 10% of the beam. The beam is then momentum analyzed by a 45° deflection through a bending magnet. A second set of copper slits transmits about half of the analyzed beam into the scattering area, where the protons then pass through a second quadrupole doublet. The doublet produces a waist in the beam at the target position over the center of the scattering stand; the size of the beam spot is typically $\frac{1}{8}$ in. by $\frac{3}{8}$ in.

After passing through the target, the beam is collected in a Faraday cup, and its charge is measured with an Elcor Model A309A current indicator and integrator. The beam collector is a 5-ft-long carbon cylinder (4-in. inner diameter and 0.5-in. wall thickness) with a 1-in.-thick carbon plate covering the far end. Carbon was chosen because its low-neutron-production results in a minimum background.⁹ The cup is preceded by a secondary electron suppressor which is maintained at -1000 V. The suppressor and collector are housed in a brass tube with a 0.002-in.-thick Kapton entrance window. The system is maintained at a pressure of 5×10^{-5} mm of mercury; this reduces the error in the charge measurement resulting from residual gas ionization to less than 0.1%. The geometry of the Faraday cup and its distance from the center of the scattering chamber are such as to assure negligible losses due to

⁵ F. H. Read and J. M. Calvert, Proc. Phys. Soc. (London) **77**, 65 (1961); S. Glashow and W. Selove, Phys. Rev. **102**, 200 (1956).

⁶ J. B. Marion, Phys. Letters **14**, 315 (1965).

⁷ J. Cerny, R. H. Pehl, and G. T. Garvey, Phys. Letters **12**, 234 (1964).

⁸ C. Detraz, J. Cerny, and R. H. Pehl, Phys. Rev. Letters **14**, 708 (1965).

⁹ Y. K. Tai, G. P. Millburn, S. N. Kaplan, and B. J. Moyer, Phys. Rev. **109**, 2086 (1958).

the multiple scattering produced by a 0.5-MeV-thick gold target in a 25-MeV proton beam. The leakage resistance of the Faraday cup was measured to be $5 \times 10^{16} \Omega$.

The energy of the beam was determined by finding the angles at which protons scattered from hydrogen have the same energies as those scattered inelastically from carbon, leaving the carbon in the 4.43- and 9.63-MeV states.¹⁰ These measurements enabled us to determine the beam energy to an accuracy of ± 0.1 MeV. However, a check of these energy measurements using a simple form of the range-energy (in aluminum) method gave somewhat higher beam energies. This discrepancy is being investigated, but it seems unlikely that the cross-over technique can be seriously in error. (*Note added in proof.* This discrepancy has been resolved; the energy of 46 MeV as originally determined by crossover technique has been found to be correct.) The energy spread of the beam was estimated to be smaller than 0.2 MeV.

B. Scattering Stand

The scattering chamber, including the targets, and the detectors were mounted on a scattering stand in the experimental area. The scattering stand consists of a central post, a circular track 3-in. wide and 8 ft. in diameter, and two arms. Each arm can be independently rotated through 360° and can be positioned with an accuracy of $\pm 0.01^\circ$; the synchro readouts associated with the arms were calibrated to $\pm 0.01^\circ$. The beam direction was determined by comparing the cross sections measured with each detector placed at a number of angles on both sides of the beam. A check of this calibration was obtained by comparing the crossover points obtained by performing the energy measurement on both sides of the beam. The direction of the beam was initially determined to within $\pm 0.03^\circ$, and subsequent checks indicated that the beam did not wander in the horizontal plane by more than $\pm 0.05^\circ$.

The scattering chamber is an aluminum housing with an outside diameter of 10.75 in. and a height of 6 in. A gap 0.75-in. high and in the median plane extends around the chamber wall through 330° . This gap is covered with a 0.002-in.-thick Kapton, which forms the exit window for the outgoing particles. The removable chamber lid contains drives and readouts for remotely positioning any one of three targets into and out of the beam and at any desired angle with respect to the direction of the beam. This angle was calibrated with an accuracy of better than 0.5° .

The following two targets were used in the present experiment: Be⁹ foil of areal density of (4.925 ± 0.020) mg cm⁻² and 1% oxygen contamination; Be⁹ foil of areal density of (23.85 ± 0.10) mg cm⁻² and 0.5% oxygen

contamination. Each foil was found to be uniform in thickness to within 2.0%.

C. Detectors and Electronics

The investigation of the elastic scattering from Be⁹ was performed using single scintillation counters. Each counter consisted of a NaI(Tl) crystal (2-in. diam, 0.5-in. thick) commercially mounted on an RCA-8053 photomultiplier tube. Each counter was held in a lead cylinder of inner diameter 2.5 in., outer diameter 7 in., and length of 10 in. The collimator assembly for each counter consisted of two slits 2 in. apart and a lead cylinder (0.875-in. inner diameter) between these for additional shielding. The solid angle for most of the measurements was $(0.815 \pm 0.004) \times 10^{-3}$ sr, and the over-all angular resolution was $\pm 0.3^\circ$.

The study of the (p,p') , (p,d) , and (p,t) reactions was carried out using a counter telescope consisting of a 500 μ m thick dE/dx surface barrier detector and one of the NaI(Tl) scintillation detector assemblies. After passing through the preamplification and amplification stages, the pulses from the surface barrier counter and scintillation counter entered a coincidence circuit-linear gate circuit arrangement; the resulting signals were then fed into an SDS 925 computer used as a two-parameter 128-channel (energy) by 32-channel (dE/dx) analyzer.

III. EXPERIMENTAL PROCEDURE, DATA REDUCTION, AND CORRECTIONS

Prerequisites for a high-precision investigation of elastic scattering and the (p,p') , (p,d) , and (p,t) reactions are (a) very low background, (b) a precise method of measuring and monitoring the incident proton beam, (c) good resolution in the energy counter, (d) good particle discrimination in the dE/dx counter, and (e) a reliable determination of the various corrections (e.g., finite geometry, multiple scattering, and reactions in the detectors).

It was felt that low background is essential not only for the study of the (p,p') , (p,d) , and (p,t) reactions but also for the investigation of elastic scattering, because of pile-up problems and uncertainties in the dead time corrections. A considerable reduction in the background was achieved by shielding all surfaces exposed to the beam, removing those surfaces more than 10 ft from the target, and shielding the detectors. In addition, the background in the region of the scattering stand due to the proton beam stopping in the Faraday cup was low because most of the beam is stopped by the carbon-plate covering the far end of the collector cylinder, the carbon plate being 7 ft from the target. This background was further reduced by shielding the rear portion of the Faraday cup by a steel cave with 6-in.-thick walls. Figure 2 shows the extent to which the background was reduced by comparing the charged particle spectra resulting from the reaction $p+C^{12}$ under the conditions (a) detectors without shielding, beam defining slits in

¹⁰ R. Smythe, Rev. Sci. Instr. 35, 1197 (1964); B. M. Bardin and M. E. Rickey, *ibid.* 35, 902 (1964).

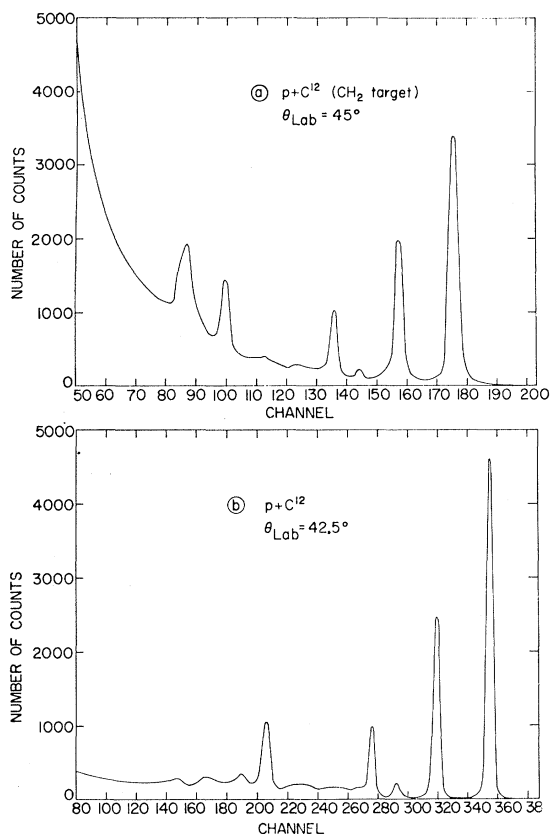


FIG. 2. Charged-particle spectra resulting from the bombardment of carbon by 46-MeV protons under the conditions: (a) detectors without shielding, beam-defining slits in front of the scattering chamber, and a small, unshielded Faraday cup close to the target, and (b) conditions as realized in the experiment.

front of the scattering chamber, and a small, unshielded Faraday cup close to the target, and (b) conditions as realized in the experiment. These latter conditions produced negligible background down to approximately 18 MeV, and even below that energy the background was quite small.

The incident beam was measured using the Faraday cup described in Sec. IIA and was monitored by one of the scintillation counters set at a fixed angle. The purpose of the monitor was to detect any inconsistency which might occur due to a malfunctioning of the integrator, poor vacuum in the Faraday cup, possible wandering of the beam, and possible deterioration of the target. Only the measurements for which the integrator and the monitor agreed to within 1% were accepted in the final analysis. Using this criterion, only 5% of the measurements were rejected, indicating that the measurement of the incident beam current was reliably performed.

The accuracy of the absolute measurements was checked by measuring absolute proton-proton cross sections using polyethylene (CH_2), hydrogen (H_2 gas), and methane (CH_4 gas) targets. The results of these

measurements were compared with predictions based on interpolations between accurate proton-proton measurements at nearby energies.¹¹ Our measurements were found to agree, to within the assigned uncertainties, with the interpolated results. They therefore provided a test for the over-all absolute measurement (integrator, solid angles, and target thickness.)

The resolution of the scintillation counters was optimized by careful selection of the detectors, design of the solid angle defining slits, and adjustment of the photomultiplier tube voltages, in particular, the focusing electrode voltage. The over-all resolution, which includes the resolution of the counter, the target thickness, the energy spread of the incident beam, and the kinematical broadening, was typically 1.5%.

The use of two parameter E - dE/dx analysis allowed simultaneous detection of proton, deuteron, and triton spectra in the energy region from 10 to 46 MeV. Figure 3 shows a dE/dx spectrum for the fixed residual energy $E_r = 25$ MeV. Discrimination between proton, deuteron, and triton groups of the same intensity and at the same residual energy was better than 1 in 10^4 . In no case was the uncertainty in the particle identification of a specific group of particles larger than 1%.

The following corrections were applied to the elastic scattering data: (a) a dead time correction for the 400-channel analyzer; (b) a correction for the occurrence of nuclear reactions in the NaI(Tl) crystals; (c) a correction for slit edge scattering; (d) multiple scattering correction; (e) finite geometry correction; (f) a correction for the elastic scatterings by the target contaminants.

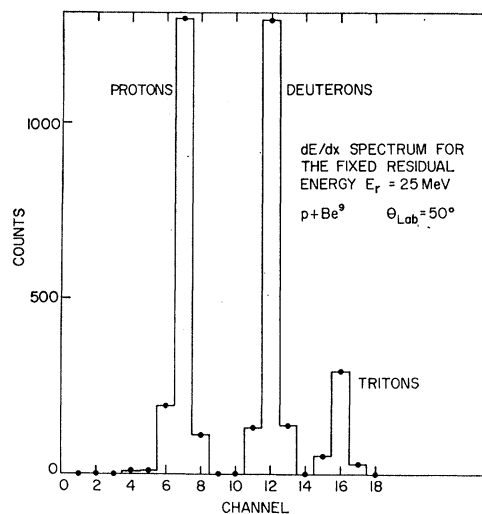


FIG. 3. A typical dE/dx spectrum for the fixed residual energy $E_r = 25$ MeV and at $\theta_{\text{Lab}} = 50^\circ$ for the reaction products of 46-MeV protons interacting with Be^9 .

¹¹ L. H. Johnston and Y. S. Tsai, Phys. Rev. **115**, 1293 (1959); C. J. Batty, G. H. Stafford, and R. S. Gilmore, Nucl. Phys. **51**, 225 (1964).

TABLE I. Corrections which were applied to the elastic-scattering data.

Type of correction	Maximum value for correction	Resulting uncertainty induced in the elastic-scattering cross section
Reactions in NaI(Tl)	+2.66%	0.5%
Multiple scattering	-0.01%	0.01%
Finite geometry	-0.89%	0.2%
Oxygen contamination	-2.13%	0.4%

Pulses from a standard pulser were simultaneously fed into the 400-channel analyzer (used for the elastic-scattering measurements) and into a scaler. The counting rates were such as to produce negligible counting losses in the scaler. The ratio of the number of pulser counts in the scaler to the number of pulser counts in the analyzer represents the analyzer dead-time correction. This value was compared with the one determined from the "live-time" meter in the analyzer and the actual time for a particular measurement. The dead-time correction never exceeded 5%, and the difference between the two independent corrections was never larger than 1%.

The above procedure was followed only during the accumulation of the elastic-scattering data. The (p,p') , (p,d) , and (p,t) data were taken with dead-time corrections as large as 15%. However, since the cross sections for these reactions were calculated relative to the elastic scattering, the uncertainty introduced by the dead-time correction was negligible.

TABLE II. Uncertainties in the elastic-scattering cross sections.

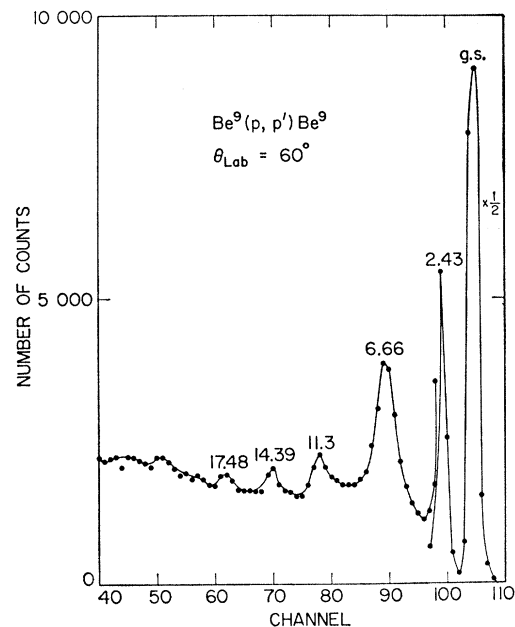
Type of uncertainty	Relative uncertainties	
	Typical value at small angles	Typical value at large angles
Counting statistics	0.2%	1.4%
Separation of elastic protons from deuterons	0.2%	None
Dead-time correction (relative)	0.5%	0.1%
Uncertainty in the scattering angle for $\theta < 20^\circ$	1.0%	Negligible
for $20^\circ < \theta < 90^\circ$	0.3%	
for $\theta > 90^\circ$		
Corrections from Table I	0.7%	0.1%
Total relative error	1.4%	1.4%
Reproducibility of the measurements	1.4%	1.4%
Absolute uncertainties		
Type of uncertainty	Value for the uncertainty	
Solid angle	0.4%	
Target thickness	2.0%	
Target composition	0.5%	
Target angle	0.1%	
Measurement of the incident beam	1.0%	
Dead-time correction (absolute)	1.0%	
Total relative error	1.4%	
Total absolute error	2.9%	

TABLE III. Uncertainties in the absolute cross sections for the (p,p') , (p,d) , and (p,t) reactions.

Reaction	Uncertainty in the absolute cross section	
	$\theta_{\text{Lab}} < 90^\circ$	$\theta_{\text{Lab}} > 90^\circ$
$\text{Be}^9(p,p')\text{Be}^{9*}$ 2.43-MeV state	<5%	<5%
$\text{Be}^9(p,d)\text{Be}^8$ ground state	10%	20%
$\text{Be}^9(p,d)\text{Be}^{8*}$ 2.90-MeV state	5%	15%
$\text{Be}^9(p,d)\text{Be}^{8*}$ 16.93-MeV state	5%	15%
$\text{Be}^9(p,d)\text{Be}^{8*}$ 17.64-MeV state	10%	20%
$\text{Be}^9(p,d)\text{Be}^{8*}$ 18.15-MeV state	10%	20%
$\text{Be}^9(p,d)\text{Be}^{8*}$ 19.05-MeV state	5%	15%
$\text{Be}^9(p,t)\text{Be}^7$ ground state	7%	20%
$\text{Be}^9(p,t)\text{Be}^{7*}$ 4.55-MeV state	7%	20%
$\text{Be}^9(p,t)\text{Be}^{7*}$ 6.51-MeV state	10%	25%
$\text{Be}^9(p,t)\text{Be}^{7*}$ 10.79-MeV state	7%	...

Any monoenergetic group of particles detected by a counter will be displayed on the analyzer as a peak plus a long tail caused by those particles which undergo nuclear reactions in the counter. This effect is insignificant at low energies, but it increases as the particle energy increases. The appropriate corrections were determined using the Minnesota and the Harvard data.¹²

An effective increase in the solid angle is produced by particles reaching the detector after penetrating a small distance through the collimator defining the solid angle of the detector, either because of their angle of incidence or because of multiple scattering by the collimator material. This process, therefore, also produces a tail in

FIG. 4. Proton spectrum resulting from 46-MeV protons bombarding Be^9 .

¹² L. H. Johnston, D. H. Service, and D. A. Swenson, IRE Trans. Nucl. Sci. NS-5, 95 (1958); D. F. Measday, Nucl. Instr. Methods 34, 353 (1965).

TABLE IV. Differential cross sections for the elastic scattering of 46-MeV protons from Be⁹.

θ_{Lab} (deg)	$\theta_{\text{c.m.}}$ (deg)	$d\sigma_{\text{Lab}}/d\Omega$ (mb/sr)	$d\sigma_{\text{c.m.}}/d\Omega$ (mb/sr)	θ_{Lab} (deg)	$\theta_{\text{c.m.}}$ (deg)	$d\sigma_{\text{Lab}}/d\Omega$ (mb/sr)	$d\sigma_{\text{c.m.}}/d\Omega$ (mb/sr)
15.0	16.7	621	501	95.0	101.6	0.280	0.288
17.5	19.5	508	412	100.0	106.6	0.204	0.214
20.0	22.3	397	323	105.0	111.4	0.148	0.158
22.5	25.1	308	251	110.0	116.3	0.115	0.126
25.0	27.8	221	181	115.0	121.0	0.0955	0.106
27.5	30.6	153	126	120.0	125.8	0.0756	0.0857
30.0	33.3	110	90.5	124.85	130.3	0.0602	0.0695
32.5	36.1	66.6	55.3	130.15	135.2	0.0502	0.0610
35.0	38.8	41.8	34.9	134.85	139.6	0.0493	0.0587
37.5	41.6	26.4	22.2	140.15	144.4	0.0442	0.0534
40.0	44.3	16.6	14.0	144.85	148.7	0.0402	0.0492
42.5	47.0	10.1	8.61	150.15	153.5	0.0380	0.0470
45.0	49.7	7.00	5.99				
47.5	52.4	5.64	4.86				
50.0	55.1	4.73	4.11				
55.0	60.5	4.13	3.64				
60.0	65.8	3.56	3.19				
65.0	71.1	2.82	2.58				
70.0	76.3	1.99	1.85				
75.0	81.5	1.35	1.28				
80.0	86.6	0.912	0.882				
85.0	91.7	0.612	0.604				
90.0	96.7	0.404	0.407				

the spectrum of a single monoenergetic group. However, since the vast majority of these particles suffer a large loss of energy, the uncertainty in the number of counts in the monoenergetic group is small. Indeed, using the formula of Burge and Smith,¹³ it was calculated that the slit-edge penetration correction to the elastic data was completely negligible for the present experiment.

However, the slit-edge penetration effect does influence the inelastic spectra. This effect is inseparable,

though, from the effects due to reactions in the detector, simultaneous multiparticle breakups, and low-energy contaminations in the incident beam. The total influence of these effects on the inelastic spectra was subtracted by drawing smooth curves through the flat minima in the various spectra. The uncertainty resulting from this procedure for any particular particle group never exceeded 10%; for the first excited state of Be⁹ this uncertainty was less than 1.0%.

TABLE V. Differential cross sections for the inelastic scattering of 46-MeV protons from the 2.43-MeV state of Be⁹.

$\theta_{\text{c.m.}}$ (deg)	$d\sigma_{\text{c.m.}}/d\Omega$ (mb/sr)	$\theta_{\text{c.m.}}$ (deg)	$d\sigma_{\text{c.m.}}/d\Omega$ (mb/sr)
16.8	6.26	101.8	0.191
19.6	6.90	106.8	0.145
22.4	7.72	111.6	0.117
25.1	8.83	116.4	0.103
27.9	9.61	121.2	0.0874
29.0	9.77	125.9	0.0812
30.7	10.0	130.6	0.0773
33.4	10.3	135.2	0.0819
36.2	10.1	139.8	0.0869
39.0	9.59	144.4	0.0811
41.7	8.59	148.9	0.0790
44.4	7.61	153.4	0.0792
47.2	6.48		
49.9	5.55		
52.6	4.57		
55.3	3.65		
60.6	2.39		
66.0	1.59		
71.2	1.11		
76.5	0.830		
81.6	0.594		
86.8	0.466		
91.8	0.357		
96.9	0.268		

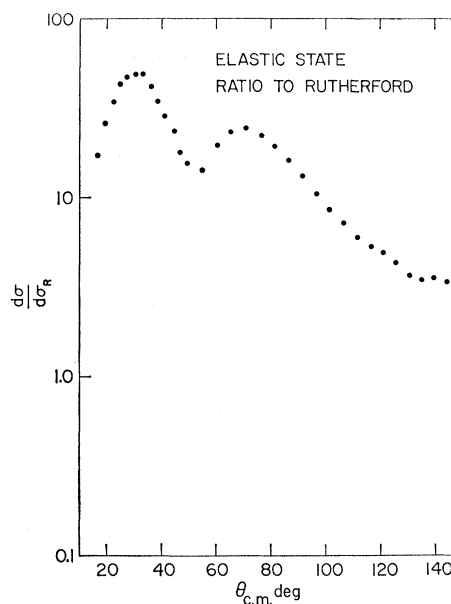


FIG. 5. The ratio of the differential elastic cross section to the Rutherford cross section as a function of scattering angle, for 46-MeV protons scattering from Be⁹. The error bars are of the size of the dots representing the data.

¹³ E. J. Burge and D. A. Smith, Rev. Sci. Instr. **33**, 1371 (1962).

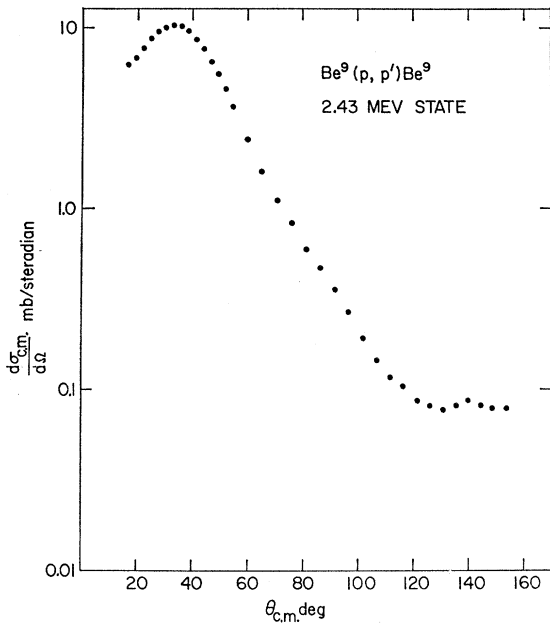


FIG. 6. The differential cross section for the inelastic scattering of 46-MeV protons from the 2.43-MeV state of Be^9 , plotted as a function of scattering angle. The error bars are of the size of the dots representing the data.

The effect due to reactions in the NaI(Tl) crystals and slit-edge penetration was investigated by measuring coincident spectra from CH_2 with two detectors set 90° apart. The collimators defining the solid angles for the two counters were chosen in such a way that the coincident events in one detector, gated by the other, fell in a region of the detector which was appreciably

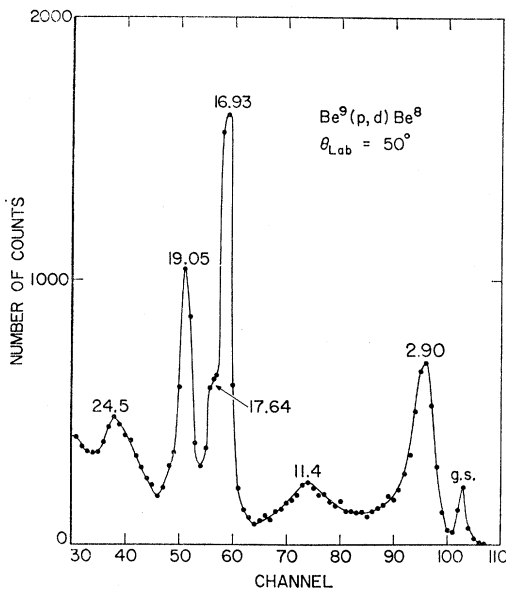


FIG. 7. Deuteron spectrum for $\theta_{\text{Lab}} = 50^\circ$ from the reaction $\text{Be}^9(p,d)\text{Be}^8$.

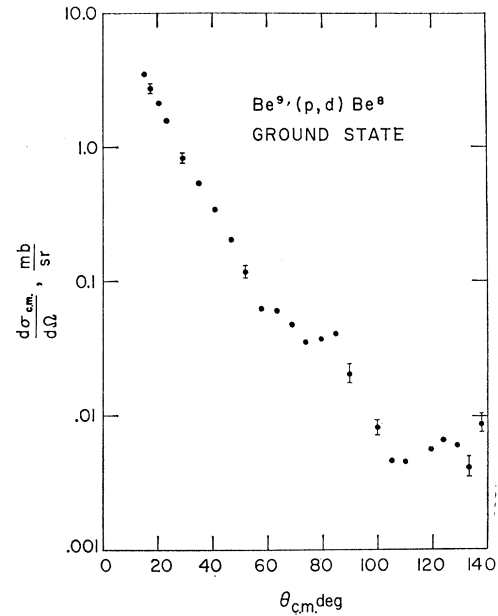


FIG. 8. Angular distribution for the reaction $\text{Be}^9(p,d)\text{Be}^8$ (ground state) for 46-MeV incident protons.

smaller than the size of its collimator; thus the gated spectrum in that detector enabled us to estimate the effect of the reactions in the NaI(Tl) crystal. The slit-penetration effects were studied using slits of various sizes. For both investigations, corrections due to the reaction $\text{C}^{12}(p,2p)\text{B}^{11}$ and due to target-out background were measured. The results of the above measurements are as follows. A value in agreement with the data of Ref. 12 was found for the effect of the reactions in the

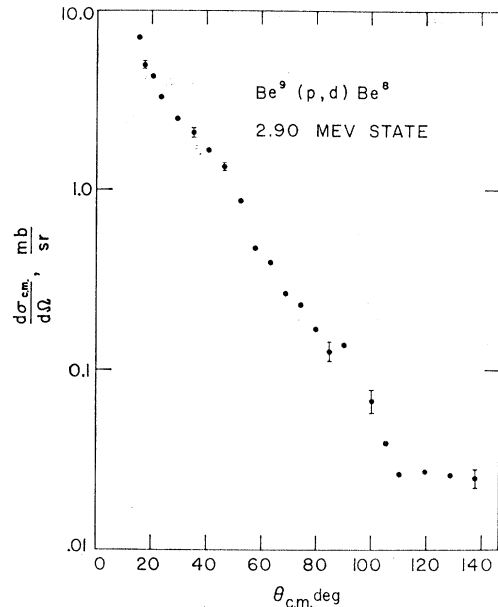


FIG. 9. Angular distribution for the reaction $\text{Be}^9(p,d)\text{Be}^{8*}$ (2.90-MeV state) for 46-MeV incident protons.

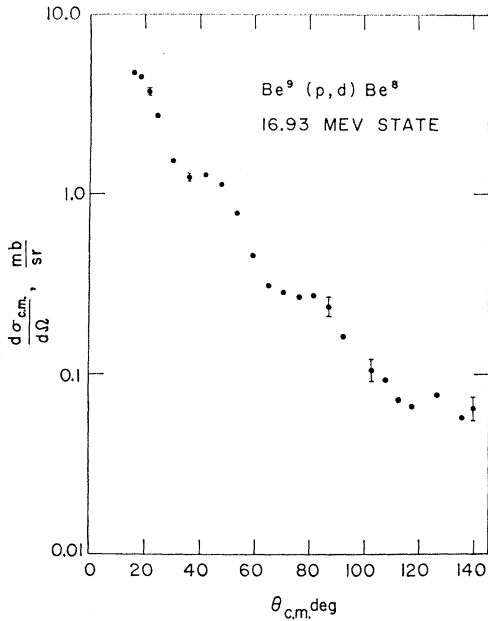


FIG. 10. Angular distribution for the reaction $\text{Be}^9(p,d)\text{Be}^{8*}$ (16.93-MeV state) for 46-MeV incident protons.

crystal; also, the slit-penetration measurements corroborate the results of Ref. 13.

The possibility of low-energy components in the incident proton beam was investigated by displaying the coincidence spectra resulting from the elastic scattering of protons from hydrogen (H_2 gas target) on our two-dimensional analyzer. While the events corresponding to the main beam component fall in one E_1E_2 point (actually a small region), the events due to

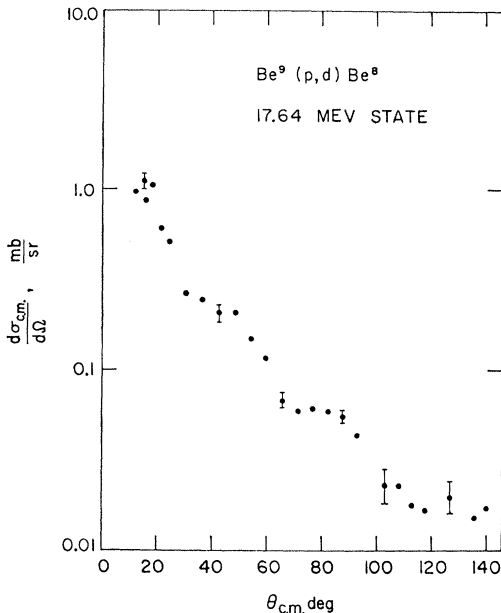


FIG. 11. Angular distribution for the reaction $\text{Be}^9(p,d)\text{Be}^{8*}$ (17.64-MeV state) for 46-MeV incident protons.

the low-energy components fall on the straight line connecting the first point and the point corresponding to $E_1=E_2=0$. As a result of such measurements, an upper limit of 1 in 10^5 was placed on the presence of low-energy particles in the incident beam.

The correction due to multiple scattering in the target was determined by using the formula of Chase and Cox,¹⁴ and it was always less than 0.01%. The smallness of this correction showed that the correction for multiple scattering in the exit window of the scattering chamber and in the air between the window and the detectors could be neglected.

Nuclear-scattering experiments are always performed with finite-sized defining collimators in front of the detectors, and a cross section of the incident beam is

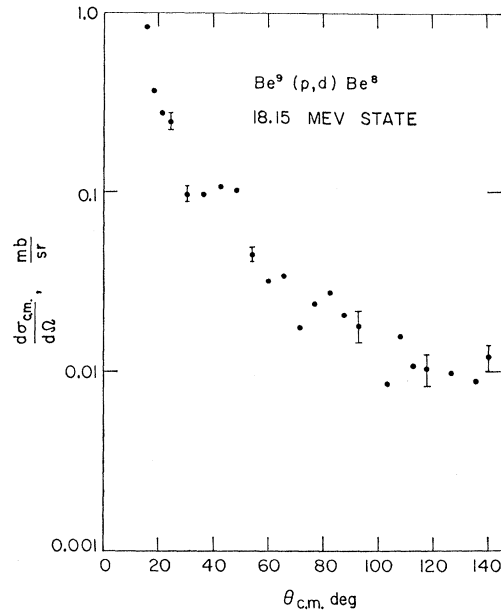


FIG. 12. Angular distribution for the reaction $\text{Be}^9(p,d)\text{Be}^{8*}$ (18.15-MeV state) for 46-MeV incident protons.

never a point. As a result, various approximations have been derived in the past to correct for these "finite geometry" effects.¹⁵ In the present experiment the beam spot at the target was produced by the last quadrupole doublet, with no beam collimators being used after the beam passes through that quadrupole. The incident beam, therefore, was not parallel, with the beam at the exit of the quadrupole acting as a source of the protons which reach the target. The correction formulas of Ref. 15 have been extended to take account of such nonparallel beams.¹⁶ The approximations on which the formula of Willmes is based are believed to yield corrections accurate to at least 10% of the value of the

¹⁴ C. T. Chase and R. T. Cox, Phys. Rev. **58**, 243 (1940).

¹⁵ I. E. Dayton and G. Schrank, Phys. Rev. **101**, 1358 (1956).

¹⁶ H. Willmes, Nucl. Instr. Methods **41**, 122 (1966); W. T. H. van Oers, G. J. C. van Niftrik, H. L. Jonkers, and K. W. Brockman, Jr., Nucl. Phys. **74**, 469 (1965).

correction itself, for the present geometry. The resulting finite geometry correction for the elastic scattering from Be^9 slightly exceeded 0.5% for a few points only, and in most cases was less than 0.2%.

The only significant contamination of the beryllium targets used in the present experiment was a small amount of oxygen. The contaminant was identified as oxygen by the angular dependence of its kinematical loss. For angles larger than 60° , the peaks due to beryllium and oxygen were completely resolved, and down to 40° the overlap was small enough so as to allow separation of the peaks by Gaussian fitting. Below 40° the number of counts to be subtracted from the beryllium was estimated by extrapolating the 30.3-MeV oxygen cross sections¹⁷ to our energy of 46 MeV. In general, this correction was less than 2%.

TABLE VI. Differential cross section for the reactions $\text{Be}^9(p,d)\text{Be}^8$ leading to the 2.90-, 16.93-, and 19.05-MeV states of Be^8 .

2.90-MeV state		16.93-MeV state		19.05-MeV state	
$\theta_{c.m.}$ (deg)	$d\sigma_{c.m.}/d\Omega$ (mb/sr)	$\theta_{c.m.}$ (deg)	$d\sigma_{c.m.}/d\Omega$ (mb/sr)	$\theta_{c.m.}$ (deg)	$d\sigma_{c.m.}/d\Omega$ (mb/sr)
15.3	7.07	15.8	4.77	12.3	1.64
17.6	4.93	18.3	4.53	15.4	1.55
20.6	4.28	21.3	3.73	16.0	1.35
23.5	3.28	24.3	2.73	18.4	1.46
29.3	2.49	30.3	1.52	21.5	1.27
35.1	2.08	36.3	1.23	24.5	1.15
40.8	1.65	42.2	1.27	30.6	0.683
46.5	1.32	48.1	1.12	36.6	0.657
52.2	0.867	53.9	0.787	42.6	0.572
57.8	0.473	59.7	0.459	48.5	0.585
63.3	0.392	65.3	0.310	54.4	0.440
68.8	0.264	70.9	0.284	60.2	0.307
74.2	0.230	76.5	0.269	71.5	0.196
79.6	0.168	81.9	0.272	82.5	0.167
84.8	0.125	87.2	0.238	93.1	0.118
90.0	0.137	92.5	0.162	103.3	0.0876
100.2	0.0670	102.6	0.104		
105.1	0.0390	107.6	0.0937		
110.0	0.0261	112.4	0.0722		
119.5	0.0272	117.2	0.0664		
128.8	0.0260	126.4	0.0768		
137.8	0.0250	135.3	0.0578		
		139.6	0.0647		

The corrections which were applied to the elastic-scattering data are summarized in Table I, and the uncertainties in the measurement of the elastic-scattering cross sections are given in Table II. Table III lists the uncertainties in the measurements of the (p,p') , (p,d) , and (p,t) reactions which were studied in the present experiment.

IV. RESULTS

A. Elastic and Inelastic Scattering

The proton spectra contained the following pronounced peaks: elastic group, 2.43-MeV state ($\Gamma=1$ MeV), 6.66-MeV state ($\Gamma=1.3$ MeV), 11.30-MeV state ($\Gamma=0.64$ MeV), 14.39-MeV state ($\Gamma=0.8$ keV), and the

¹⁷ B. W. Ridley and J. F. Turner, Nucl. Phys. **58**, 497 (1964).

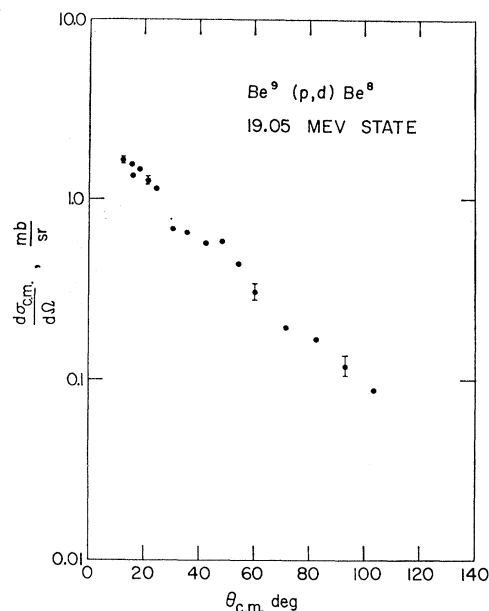


FIG. 13. Angular distribution for the reaction $\text{Be}^9(p,d)\text{Be}^{8*}$ (19.05-MeV state) for 46-MeV incident protons.

17.48-MeV state ($\Gamma=0.05$ MeV). Figure 4 shows a typical proton spectrum, with $\theta_{\text{lab}}=60^\circ$. A careful analysis of the spectra was carried out in the following manner. First, a subtraction was made of the continuum which is associated with the multibody breakups and with the "tails" associated with the elastic scattering. Second, Gaussian curves were fit to the remaining structure, with the widths of the groups being determined by folding in the experimental resolution and the widths as given above.

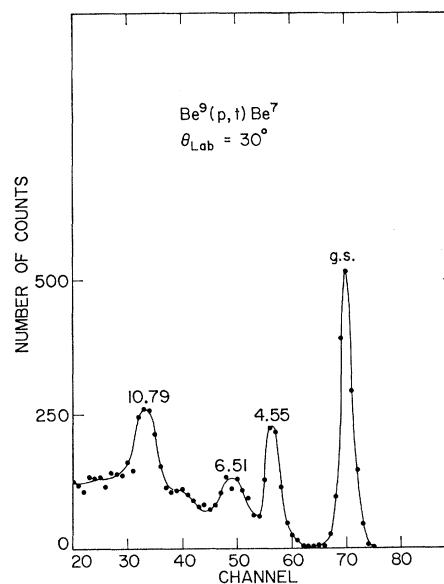


FIG. 14. Triton spectrum for $\theta_{\text{Lab}}=30^\circ$ from the reaction $\text{Be}^9(p,t)\text{Be}^7$.

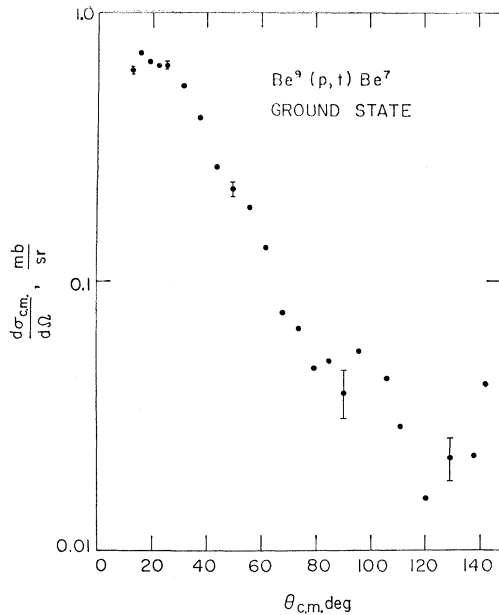


FIG. 15. Angular distribution for the reaction $\text{Be}^9(p,t)\text{Be}^7$ (ground state) for 46-MeV incident protons.

The multibody-breakup spectra were determined essentially by the regions in the spectra which had no peaks and by the valleys in between peaks. These points were connected by a smooth curve which was extrapolated to zero at the energy corresponding to the highest energy resulting from a multibody breakup reaction. This procedure was used for the analysis of the proton, deuteron, and triton spectra. The resulting proton multibody spectra are compatible with the simultaneous breakup mechanism. In addition to the above mentioned groups, the analysis of the proton

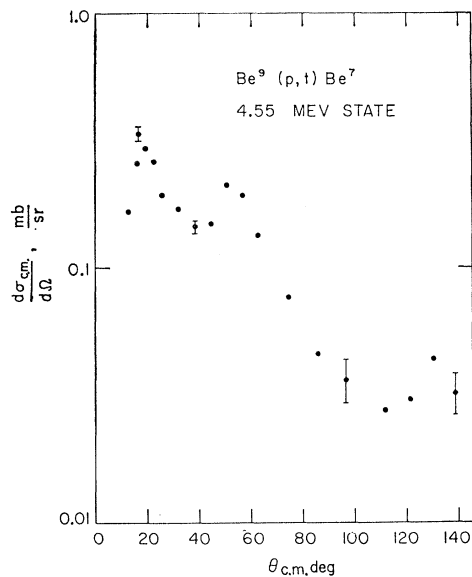


FIG. 16. Angular distribution for the reaction $\text{Be}^9(p,t)\text{Be}^{7*}$ (4.55-MeV state) for 46-MeV incident protons.

spectra revealed levels in Be^9 at 4.7 MeV and at 7.9 MeV.

The angular distributions for the elastic scattering and the inelastic scattering from the 2.43 MeV state of Be^9 are given in Tables IV and V and in Figs. 5 and 6.

B. (p,d) Reactions

The deuteron spectra contained pronounced peaks corresponding to the following levels in Be^8 : ground state, 2.90-MeV state ($\Gamma=1.45$ MeV), 11.4-MeV state ($\Gamma=7$ MeV), 16.93-MeV state ($\Gamma=0.09$ MeV), 17.64-MeV state ($\Gamma=0.01$ MeV), 18.15-MeV state ($\Gamma=0.15$ MeV), 19.05-MeV state ($\Gamma=0.27$ MeV), and a group

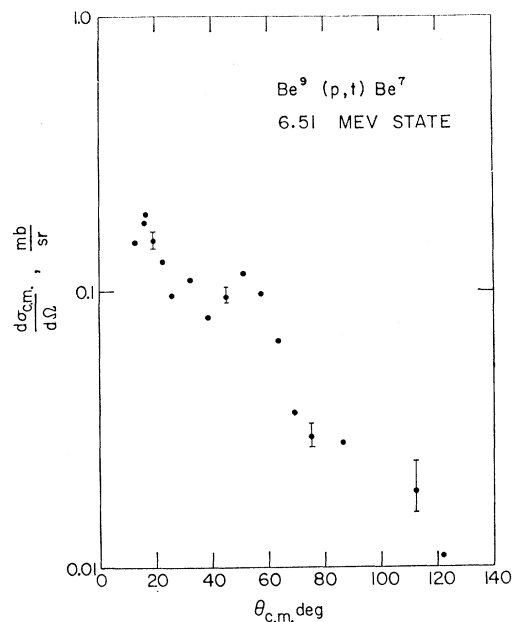


FIG. 17. Angular distribution for the reaction $\text{Be}^9(p,t)\text{Be}^{7*}$ (6.51-MeV state) for 46-MeV incident protons.

at about 24.5 MeV. A deuteron spectrum corresponding to the laboratory scattering angle 50° is shown in Fig. 7.

At each angle the 11.4-MeV group appeared as a very broad group superimposed on a continuum, and it was felt that the error associated with the subtraction procedure would make it hardly worthwhile to analyze. Of all the deuteron groups, the 2.9-MeV group and the 16.9-MeV group were the most prominent. A group which could be associated with the 16.63-MeV state appeared as a shoulder (on the 16.9-MeV peak) only at $\theta_{\text{lab}}=70^\circ$.¹⁸ At this angle, it was estimated that the intensity of the 16.6-MeV group is approximately 5% of that of the 16.9-MeV group. We were unable to separate the 16.6-MeV group from the 16.9-MeV group, and the cross sections quoted for the 16.9-MeV group include the contribution from the 16.6-MeV group.

The particularly pronounced yield associated with the 16.9-MeV level can be readily explained in terms of

¹⁸ J. B. Marion, C. A. Ludemann, and P. G. Roos, Phys. Letters 22, 172 (1966).

the configuration suggested by Marion.⁶ (See Sec. I.) When the nucleus Be^8 is left in the 16.9-MeV state, the reaction $p+\text{Be}^9$ is said to be represented by the configuration $p+\{n+[n+\text{Be}^7(\text{gnd. state})]\}$, and the transition corresponds to the pickup of a neutron from Be^8 , leaving Be^7 with the other neutron to make up the 16.9-MeV state of Be^8 . The weak excitation of the 16.6-MeV level is a result of the $(p+\text{Li}^7)$ configuration for that level. However, the small cross section which we measured for the 18.15-MeV level suggests that this level does not have the configuration $[n+\text{Be}^{7*}$ (0.43-MeV state)].

The cross sections measured in the present experiment for the most prominent deuteron groups (ground state, 2.9-MeV state, and 16.9-MeV state) were found

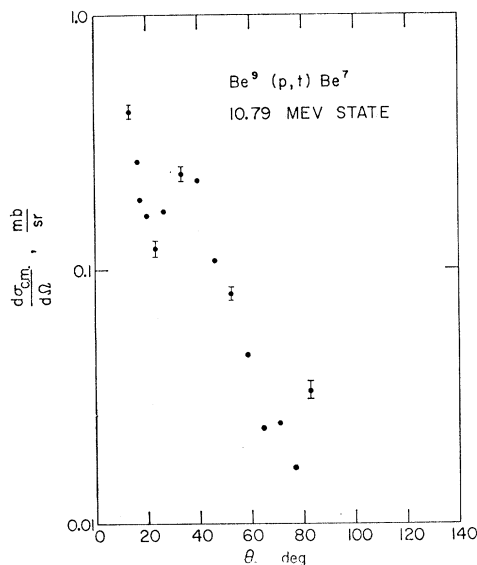


FIG. 18. Angular distribution for the reaction $\text{Be}^9(p,t)\text{Be}^{7*}$ (10.79-MeV state) for 46-MeV incident protons.

to be somewhat different from those which have been reported by Marion, *et al.*¹⁸ and by Short,⁴ both experiments being near 40 MeV. We therefore investigated the $\text{Be}^9(p,d)\text{Be}^8$ reaction for 40-MeV incident protons and found cross sections in agreement with those of Ref. 4 and 18. The reaction was then further investigated in this laboratory at 36 MeV¹⁹; the data indicate that in the region from 36 to 46 MeV, the cross section of the ground-state group decreases by a factor of 2, the cross section of the 2.9-MeV group also decreases, while the 16.9-MeV group cross section slowly increases, by approximately 30%.

Angular distributions for the ground state, 2.90-MeV state, 16.93-MeV state, 17.64-MeV state, 18.15-MeV state, and 19.05-MeV state groups are given in Figs. 8–13. The differential cross sections for the 2.90-MeV state, 16.93-MeV state, and 19.05-MeV state groups are tabulated in Table VI.

¹⁹ T. A. Cahill (private communication).

TABLE VII. Differential cross sections for the reactions $\text{Be}^9(p,t)\text{Be}^7$ leading to the ground state, the 4.55-MeV state, and the 10.79-MeV state of Be^7 .

Ground state		4.55-MeV state		10.79-MeV state	
$\theta_{c.m.}$ (deg)	$d\sigma_{c.m.}/d\Omega$ (mb/sr)	$\theta_{c.m.}$ (deg)	$d\sigma_{c.m.}/d\Omega$ (mb/sr)	$\theta_{c.m.}$ (deg)	$d\sigma_{c.m.}/d\Omega$ (mb/sr)
12.6	0.612	12.9	0.166	13.3	0.418
15.8	0.713	16.1	0.254	16.7	0.265
16.4	0.752	16.7	0.335	17.3	0.188
18.9	0.660	19.3	0.292	20.0	0.163
22.1	0.635	22.5	0.259	23.3	0.121
25.2	0.639	25.7	0.192	26.6	0.169
31.4	0.533	32.0	0.170	33.1	0.237
37.6	0.404	38.3	0.144	39.6	0.223
43.8	0.264	44.5	0.148	46.1	0.108
49.8	0.220	50.7	0.210	52.4	0.0803
55.8	0.187	56.8	0.192	58.7	0.0461
61.7	0.133	62.8	0.133	64.9	0.0237
67.6	0.0767	74.5	0.0766	70.9	0.0249
73.3	0.0669	85.7	0.0457	76.9	0.0167
78.9	0.0476	96.5	0.0362	82.7	0.0334
84.4	0.0504	111.7	0.0275		
89.8	0.0385	121.2	0.0301		
95.1	0.0550	130.2	0.0436		
105.4	0.0436	138.7	0.0320		
110.3	0.0290				
119.8	0.0156				
128.9	0.0221				
137.5	0.0226				
141.7	0.0413				

C. (p,t) Reactions

The triton spectra contained pronounced peaks corresponding to the following levels in Be^7 : ground state, 4.55-MeV state ($\Gamma=0.1$ MeV), 6.51-MeV state ($\Gamma=1.20$ MeV), and 10.79-MeV state ($\Gamma=0.3$ MeV). The ground-state group could not be separated from the group corresponding to the 0.431-MeV state; on the basis of the work of Detraz *et al.*,⁸ it is felt that this state contributed less than 20% to what is referred to as the ground state group in this paper.

Fig. 14 is a triton spectrum for the laboratory angle 30° . Angular distributions for the four measured triton

TABLE VIII. Summary of the reactions induced by the bombardment of Be^9 by 46-MeV protons studied in the present experiment.

Reaction	Peak cross section (mb/sr)
$\text{Be}^9(p,p')\text{Be}^{9*}$ (2.43-MeV state)	10.3
$\text{Be}^9(p,p')\text{Be}^{9*}$ (6.66-MeV state)	9.0
$\text{Be}^9(p,p')\text{Be}^{9*}$ (11.30-MeV state)	1.25
$\text{Be}^9(p,p')\text{Be}^{9*}$ (14.39-MeV state)	0.77
$\text{Be}^9(p,p')\text{Be}^{9*}$ (17.48-MeV state)	0.21
$\text{Be}^9(p,d)\text{Be}^8$ (Ground state)	3.5
$\text{Be}^9(p,d)\text{Be}^{8*}$ (2.90-MeV state)	7.1
$\text{Be}^9(p,d)\text{Be}^{8*}$ (16.93-MeV state)	4.8
$\text{Be}^9(p,d)\text{Be}^{8*}$ (17.64-MeV state)	1.1
$\text{Be}^9(p,d)\text{Be}^{8*}$ (18.15-MeV state)	0.84
$\text{Be}^9(p,d)\text{Be}^{8*}$ (19.05-MeV state)	1.5
$\text{Be}^9(p,t)\text{Be}^7$ (Ground state)	0.75
$\text{Be}^9(p,t)\text{Be}^{7*}$ (4.55-MeV state)	0.34
$\text{Be}^9(p,t)\text{Be}^{7*}$ (6.51-MeV state)	0.19
$\text{Be}^9(p,t)\text{Be}^{7*}$ (10.79-MeV state)	0.42

groups are given in Figs. 15–18, and Table VII lists the differential cross sections for the ground state, the 4.55-MeV state, and the 10.79-MeV state groups. The latter group has been recently studied by Detraz, *et al.*⁸ at 43.7 MeV. Though the angular distributions agree remarkably well in shape, there exists a difference in the absolute cross sections which is hard to attribute to such a small difference in the incident energy.

D. Summary

Table VIII gives a summary of the reactions induced by the bombardment of Be⁹ by 46-MeV protons studied in the present experiment. The simultaneous measurement of proton, deuteron, and triton spectra enabled us to accumulate the data with reasonable speed and to

determine the absolute cross sections with increased accuracy.

Optical-model and distorted-wave Born-approximation calculations of the present data will be reported in a separate paper.

ACKNOWLEDGMENTS

The authors wish to express their gratitude to M. Chronoviat and to C. Casillas, who designed and built the experimental apparatus, respectively, to M. Smith who wrote the computer programs which assisted in the accumulation and reduction of the data, to H. Preston for his work on the electronic apparatus, and to the senior cyclotron staff of S. Plunkett and G. Jones for their assistance in the maintenance of the cyclotron.

Four-Quasiparticle Excitations and Two-Phonon Vibrational States in Spherical Nuclei. Even-Parity States of Even Tin Isotopes

P. L. OTTAVIANI*

Istituto di Fisica dell'Universita di Bologna, Bologna, Italy

AND

M. SAVOIA†

*Istituto di Fisica dell'Universita di Bologna, Bologna, Italy;
and Centro de Investigacion y de Estudios Avanzados del I.P.N., Mexico*

AND

J. SAWICKI‡

*Laboratoire Joliot-Curie de Physique Nucleaire, Orsay, France;
and Centro de Investigacion y de Estudios Avanzados del I.P.N., Mexico*

AND

A. TOMASINI§

Istituto di Fisica dell'Universita di Bologna, Bologna, Italy

(Received 2 June 1966)

A microscopic theory of the low-lying states of even-even spherical nuclei is developed in which eigenvectors are linear combinations of two- and four-quasiparticle excitations. The quasiparticles are defined by the Bogoliubov-Valatin canonical transformation. The method is called the quasiparticle second Tamm-Dancoff (QSTD) approximation, since no ground-state correlations are included. It is found that the spurious kets due to the particle-number nonconservation must be absolutely projected out of the secular matrices before their diagonalization. Such a procedure is described and applied. Formulas are given for the electromagnetic transition probabilities. The theory is applied to the study of the 2^+ , 4^+ , and 0^+ states of the even tin isotopes. The single-particle radial wave functions employed are those of a Saxon-Woods potential and of a harmonic-oscillator potential. The two-nucleon residual interaction potential is spin-dependent and of zero range. Satisfactory numerical agreement with the observed 2^+ and 4^+ low-lying levels is obtained with the Saxon-Woods wave functions for a reasonable strength constant of our zero-range force. Appreciable admixtures of the four-quasiparticle creation components are found even in the lowest lying levels. Poor agreement is obtained for the 0^+ states, for which a more refined theory is necessary (rather unreasonable values of the strength constant of the zero-range potential are required to fit the 0^+ data). Generally, markedly worse 2^+ results are obtained if we replace the Saxon-Woods wave functions with harmonic-oscillator wave functions.

1. INTRODUCTION

RECENTLY, microscopic theories have been proposed for two-phonon-type vibrational states of spherical "superconductor" nuclei in a paper by

by three of us¹ (hereafter referred to as I), and in papers by Tamura and Udagawa² and by Hsu and French.³ In the formalism of these papers the two-

* Present address: Centro di Calcolo del Comitato Nazionale per l'Energia Nucleare, Bologna, Italy.

† Present address: Istituto di Fisica di Bologna, Bologna, Italy.

‡ Present address: CERN, Geneva, Switzerland.

§ Deceased on June 15, 1965.

¹ M. Savoia, J. Sawicki, and A. Tomasini, *Nuovo Cimento* **32**, 991 (1964); this reference contains numerous misprints, and we present here several of the equations of I in their corrected form.

² T. Tamura and T. Udagawa, *Nucl. Phys.* **53**, 33 (1964).

³ L. S. Hsu and J. B. French, *Phys. Letters* **19**, 135 (1965); cf. also N. Auerbach, *ibid.* **21**, 57 (1966).